FEMS Microbiology Ecology, 96, 2020, fiaa151

doi: 10.1093/femsec/fiaa151
Advance Access Publication Date: 5 August 2020
Research Article

RESEARCH ARTICLE

PbS biomineralization using cysteine: *Bacillus cereus* and the sulfur rush

Lucian C. Staicu[1,*], Paulina J. Wojtowicz[1], Mihály Pósfai[2], Péter Pekker[3], Adrian Gorecki[1], Fiona L. Jordan[4] and Larry L. Barton[4]

[1]Faculty of Biology, University of Warsaw, Miecznikowa 1, 02-096 Warsaw, Poland, [2]Department of Earth and Environmental Sciences, University of Pannonia, Egyetem u. 10, H-8200, Veszprém, Hungary, [3]Research Institute of Biomolecular and Chemical Engineering, University of Pannonia, Egyetem u. 10, H-8200, Veszprém, Hungary and [4]Department of Biology, University of New Mexico, MSCO3 2020, Albuquerque, NM 87131, USA

*Corresponding author: University of Warsaw, Miecznikowa 1, Warsaw 02–096, Poland. Tel: +48-22-55-41-302; E-mail: staicu@biol.uw.edu.pl

One sentence summary: This article describes a novel strategy employed by bacteria to reduce the toxicity of lead by forming a mineral with limited solubility.

Editor: John Stolz

ABSTRACT

Bacillus sp. Abq, belonging to *Bacillus cereus* sensu lato, was isolated from an aquifer in New Mexico, USA and phylogenetically classified. The isolate possesses the unusual property of precipitating Pb(II) by using cysteine, which is degraded intracellularly to hydrogen sulfide (H_2S). H_2S is then exported to the extracellular environment to react with Pb(II), yielding PbS (galena). Biochemical and growth tests showed that other sulfur sources tested (sulfate, thiosulfate, and methionine) were not reduced to hydrogen sulfide. Using equimolar concentration of cysteine, 1 mM of soluble Pb(II) was removed from Lysogeny Broth (LB) medium within 120 h of aerobic incubation forming black, solid PbS, with a removal rate of 2.03 μg L^{-1} h^{-1} (~8.7 μM L^{-1} h^{-1}). The mineralogy of biogenic PbS was characterized and confirmed by XRD, HRTEM and EDX. Electron microscopy and electron diffraction identified crystalline PbS nanoparticles with a diameter <10 nm, localized in the extracellular matrix and on the surface of the cells. This is the first study demonstrating the use of cysteine in Pb(II) precipitation as insoluble PbS and it may pave the way to PbS recovery from secondary resources, such as Pb-laden industrial effluents.

Keywords: *Bacillus cereus*; lead (Pb); cysteine; galena (PbS); biominerals

INTRODUCTION

Lead (Pb) ranks as a major anthropogenic pollutant, with mining industry and fossil fuel burning for energy production as major contributors (Needleman 2004; Rumble 2018). Because Pb is rarely found in nature as a pure element, its industrial production is based on the mineral galena (PbS). Various industrial activities, including the production of batteries, ammunition, plumbing, alloys, lead crystal glassware, shields for X-ray equipment and nuclear reactors, employ Pb as a raw material (Rumble 2018). All these products ultimately release lead to the environment contributing to its mobilization through geospheres. An important aspect adding to Pb pollution is the historical heritage related to its use as an anti-knock additive in gasoline and to mining activities (Mills, Simpson and Adderley 2014; Finlay *et al.* 2021). Although tetraethyllead, $(CH_3CH_2)_4Pb$, a petro-fuel additive used on large scale as an effective octane rating booster, has been phased out, its legacy still persists in terrestrial and aquatic ecosystems (Wedge 1999). Unlike organic pollution, metals (including Pb) do not degrade (mineralize) in the environment and thus accumulate over time.

Received: 17 May 2020; **Accepted:** 28 July 2020

Pb does not possess any known biological function and the lead ion, Pb(II), is highly toxic. Pb has detrimental effects on protein synthesis and leads to alteration of the osmotic balance, enzyme inhibition, nucleic acid damage, disruption of membrane functions and oxidative phosphorylation (Bruins, Kapil and Oehme 2000). Lead is neurotoxic and is associated with learning disabilities (Canfield *et al.* 2003). In bacteria, Pb(II) is suggested to cross the plasma membrane by nonspecific uptake pathways for Mn(II) and Zn(II) (Bruins, Kapil and Oehme 2000). In certain cases, free Pb(II) does not accumulate in the cytoplasm because it is pumped out from the cell by export systems using P-type ATPases (Rensing *et al.* 1998). These transporters are distributed throughout Bacteria domain and include CadA, ZntA, and PbrA (Jaroslawiecka and Piotrowska-Seget 2014). Other intracellular proposed detoxification strategies include binding of Pb(II) to metallothioneins and precipitating it as insoluble phosphates (Dopson *et al.* 2003). However, this strategy comes with important costs in terms of energy (efflux systems), materials, and the challenge to store and handle solid inclusions intracellularly. A better alternative is to keep Pb out of the cell in a non-bioavailable, low-solubility form, such as phosphates, precipitated in extracellular polysaccharides, and polymers naturally occurring in the cell wall (Dopson *et al.* 2003).

From an environmental perspective, Pb biomineralization as insoluble minerals is desirable because this process limits its mobility (Roane 1999). Apart from phosphates, sulfides (S^{2-}) are known to form highly insoluble minerals. For instance, PbS has a low solubility constant product (K_{sp}) of 3.2×10^{-28} (Rumble 2018), which renders it non bioavailable. Sulfide precipitation of metals is less pH sensitive than other metal precipitates, thus being a process active under a wide range of geochemical conditions (Fu and Wang 2011). Sulfate reducing bacteria (SRB) play a key role in the conversion of high valence state sulfur (e.g. SO_4^{2-}) to S^{2-} (Muyzer and Stams 2008; Barton and Fauque 2009). Understanding the behavior of Pb and the generation of sulfide by bacteria is critical not only for the environment but also for human health. Such was the case of Pb poisoning in Flint, Michigan, where the change in drinking water chemistry had a direct impact on Pb release from the aging water supply system (Roy and Edwards 2018). However, the use of low-valence state sulfur for the precipitation of lead as PbS has been marginally investigated. This is particularly relevant since low-valence states biomolecules (e.g. cysteine and methionine) are present in all bacteria and are a readily available source of sulfide for Pb detoxification.

The aim of this study was to evaluate the immobilization of Pb(II) by a bacterial strain able to produce hydrogen sulfide from cysteine and to characterize the PbS biomineralization product. The specific objectives were to (i) identify if cysteine is the sole sulfide-source for PbS precipitation, (ii) establish if the biomineralization process of PbS is intra- or extracellular and (iii) propose a model for cysteine utilization and PbS biomineralization in the investigated bacterial strain.

MATERIALS AND METHODS

Bacterial strain isolation

The bacterial strain was isolated from an aquifer in New Mexico, USA (middle of the Rio Grande valley; Latitude: 35.106766 °N, Longitude: −106.629181°W) by Prof. Larry Barton and his team at New Mexico University. The water sample was taken from well water drawn at 381 m below the surface.

Phylogeny

Total DNA extraction of the isolate was done using a Genomic Mini Kit (A & A Biotechnology, Gdynia, Poland) according to the manufacturer's instructions. The DNA concentration was determined using the Qubit™ 2.0 Fluorometer (Invitrogen, Carlsbad, CA, USA). About 10 ng of extracted DNA were used as a template for amplification of 16S rRNA gene. Reaction was prepared using KAPA HiFi polymerase in a final concentration of 0.5 U (KAPA Biosystems) and 0.3 μM of universal primers (27F: AGAGTTTGATCMTGGCTCAG, 1492R: GGTTACCTTGTTACGACTT). Annealing was performed at 63°C and a total of 27 cycles were used (Mastercycler Nexus GX2 thermocycler, Eppendorf). Three technical replicates were pooled, purified by Clean up Purification Kit (EURx, Gdansk, Poland) and sent for sequencing (Oligo.pl, Polish Academy of Science, Warsaw, Poland).

For the phylogenetic classification of the isolate a molecular approach utilizing sequencing of the 16S rRNA gene was applied. A phylogenetic analysis based on the 16S rRNA gene sequence of the isolate and 100 other reference *Bacillus* species was performed using the Maximum Likelihood method and Tamura-Nei model (Tamura and Nei 1993). Phylogenetic tree was constructed using MEGA-X software (Kumar *et al.* 2018) involving additional 99 16S rRNA originated from *Bacillus* spp. strains deposited in NCBI database (as of 15 December 2019). This analysis involved 101 nucleotide sequences including 16S rRNA sequence of *Clostridium botulinum* 202F used as an outlier. There were a total of 1367 positions in the final dataset. Evolutionary analyses were conducted in MEGA X (Kumar *et al.* 2018). Initial tree(s) for the heuristic search were obtained automatically by applying Neighbor-Join and BioNJ algorithms to a matrix of pairwise distances estimated using the Maximum Composite Likelihood (MCL) approach, and then selecting the topology with superior log likelihood value. A discrete Gamma distribution was used to model evolutionary rate differences among sites (five categories (+G, parameter = 0.1132)).

Biochemical characterization

API 20E and 20NE strips were used to determine the biochemical profile of the strain according to the manufacturer's instructions (BioMérieux). Triple Sugar Iron (TSI) Agar slants were prepared in the lab and contained agar 1.2%, peptone 2%, meat extract 0.3%, phenol red 25 mg L^{-1} (a pH-sensitive dye), lactose 1%, sucrose 1%, glucose 0.1%, yeast extract 0.3%, NaCl 0.5%, sodium thiosulfate 0.3%, and ferrous sulfate 0.2%, pH 7.4 (adapted from Sigma 2020). API 20E and 20NE, and TSI were performed in triplicate. Oil displacement activity assay was performed to assess the capacity of the strain to produce surfactants (this technique measures the diameter of clear zones on an oil-water surface resulted from dropping of a solution containing biosurfactant) (Morikawa 2006). In short, 50 μL of diesel oil containing Sudan red dye were added to a Petri dish containing distilled water. A drop of the supernatant and the unfiltered culture of the strain grown in LB and in LB + Pb + cysteine was added to the Petri dish, and the spreading of the oil was observed. A drop of a *Bacillus subtilis* ANT_WA51 culture was used as control.

Incubations and reagents

Aerobic incubations:
Investigations on the capacity of the strain to metabolize lead and cysteine were carried out in Lysogeny Broth (LB). LB medium (from BioMaxima) contained tryptone 10 g L^{-1}, yeast extract,

5 g L^{-1}, NaCl 5 g L^{-1}. LB medium was adjusted to pH 5 and autoclaved. Stock solutions of lead acetate trihydrate—hereafter Pb(II)—and of *L*-cysteine-HCl monohydrate (Sigma) were filter-sterilized using 0.2 μm pore diameter Acrodisc PF filters (Gelman Sciences, USA) and added aseptically to the growth medium as indicated to give final concentrations of total 1 mM of each. Due to the nature of the LB medium, an organically-rich solution, the soluble Pb(II) concentration can vary from one incubation to another. However, the results indicated a limited variation between independent experiments (±10–15%). To circumvent this limitation, the initial Pb(II) concentration (t_0) was measured for all experiments and was used to calculate the Pb(II) removal rates. The flasks were inoculated with 1% of a stock culture of *Bacillus* sp. Abq and the incubation was carried out at 30°C on a rotary shaker at 150 rpm, in the dark. The initial pH value was set to 5.0 using 1 N HCl acid. The reason was the tendency of the pH to increase by around two units during incubation, reaching around 7.5 at the end of the experiment. Based on a pilot experiment, above pH 8 lead starts to precipitate from solution.

Anaerobic incubations:
Anaerobic incubations were performed in LB. 80 mL of sterile LB medium were added aseptically to serum bottles (120 mL), which were then crimp-sealed with butyl rubber septa and aluminum caps, and the headspace was flushed with nitrogen gas for 5 min through a 0.22 μm filter to ensure sterility. The incubations were performed at 30°C, pH 7.0, in the dark on a rotary shaker at 150 rpm. In order to better visualize the formation of the precipitate, after 48 h of incubation homogenous samples were taken and centrifuged in microcentrifuge tubes.

Electron microscopy

Samples for transmission electron microscopy (TEM) were prepared by depositing a drop of the cell suspension on copper TEM grids covered by an ultrathin amorphous carbon film. TEM analyses were performed using a Talos F200X G2 instrument (Thermo Fisher), operated at 200 kV accelerating voltage, equipped with a field-emission gun and a four-detector Super-X energy-dispersive X-ray spectrometer, and capable of working in both conventional TEM and scanning transmission (STEM) modes. Low-magnification bright-field (BF) images, high-resolution (HRTEM) images and selected-area electron diffraction (SAED) patterns were obtained in TEM mode. In addition, bright- and dark-field images were also obtained in STEM mode. Elemental compositions were determined using energy-dispersive X-ray spectrometry (EDS).

Lead (Pb) measurement and PbS analysis

Bacillus sp. Abq was grown in LB medium supplemented with 1 mM lead acetate and 1 mM *L*-cysteine or lead-containing LB medium without *L*-cysteine. The lead concentration was chosen based on literature reporting concentrations up to 1.5 mM Pb(II) in environmental samples associated with acid mine drainage (Campaner *et al.* 2014). We used equimolar and 3:1 concentrations of cysteine to Pb(II) in order to obtain stoichiometric removal and to demonstrate the impact of cysteine on increasing Pb(II) removal rates, respectively. Control experiments were performed to determine the potential abiotic interaction between Pb and cysteine. Another experiment assessed whether the degradation of cysteine was intra- or extracellular. For this, the supernatant of a *Bacillus* sp. Abq culture grown using the same incubation conditions in LB medium amended with 1 mM cysteine was recovered, filter-sterilized and inoculated with 1 mM Pb(II), and with 1 mM Pb(II) + 1 mM cysteine. Cultures were inoculated and incubated on the shaker at 30°C for 7 days. Samples were removed from the flasks at various time points (12, 24, 48, 72, 96 and 120 h), centrifuged at 6000 × *g* for 10 min, and the supernatant was analyzed for lead after it was filtered through a Nucleopore filter with a pore diameter of 0.22 μm. The specific Pb(II) reduction rate was calculated from the slope of the linearized time course. The experiments were performed in triplicate.

Pb was measured by Flame Atomic Absorption Spectroscopy (FAAS) using a Thermo Scientific—SOLAAR M Series and a gas mixture of air and acetylene. The calibration curve range was 0–10 mg L^{-1} and the lower limit of quantification was 0.01 mg L^{-1}.

PbS: The mineral composition of the investigated samples was obtained via powder X-ray diffraction (XRD) by using a SmartLab RIGAKU diffractometer with graphite-monochromatized CuK radiation operating at 9 kV. The measurements were conducted at 2–75° 2θ (depending on the measurement) with a measuring step of 0.05°2θ/s. The XRD patterns were interpreted using the XRayan program (Version 4.2.2).

RESULTS AND DISCUSSION

Phylogenetic classification of the isolate

Based on these results, the isolate was classified as *Bacillus* sp. Abq (Abq from Albuquerque, New Mexico). The accession number obtained for *Bacillus* sp. Abq is MT072324. The results (Fig. 1) indicate that the isolate is most closely related to *Bacillus cereus* (99.79% similarity) and to *B. thuringiensis* (99.79% similarity), which cluster together and belong to the *Bacillus cereus* sensu lato group (Jensen *et al.* 2003).

Morphology and biochemical characterization

On LB medium, *Bacillus* sp. Abq forms round, off-white colonies, with clear edges, ∼5 mm across. The strain is aerobic, showing limited anaerobic growth (Fig. S1, Supporting Information).

The use of API test kits (20E and 20 NE) revealed that the strain can use a wide range of substrates such as citrate, arginine, tryptophan, gelatin, esculin, and glucose (aerobically and via fermentation) (Table S1, Supporting Information). In addition, *Bacillus* sp. Abq reduces nitrate to nitrite, and uses various carbohydrates including maltose, gluconate and maltose. On the other hand, it cannot degrade urea, does not produce indole or H_2S (from thiosulfate, S_2O_3) and it cannot use a number of carbohydrates such as mannitol, inositol and saccharose.

The biochemical analysis was complemented by performing the Triple Sugar Iron (TSI) test (Fig. S1, Supporting Information). The bottom of the tube turned yellow, indicative of glucose fermentation. The fact that no darkening appeared in the inoculated tube revealed the incapacity of *Bacillus* sp. Abq to reduce sulfate and thiosulfate to hydrogen sulfide, that would have reacted with the Fe(II) present in the medium by forming a black iron sulfide mineral precipitate.

Numerous *Bacillus* species have been reported for their capacity to produce various surfactants such as surfactin, iturin A, polymixins and lipopeptides (Jahan *et al.* 2020). In order to check the possibility of an extracellular interaction of bacterial products with cysteine and Pb(II), the production of surfactants by the isolate was tested using the oil displacement activity

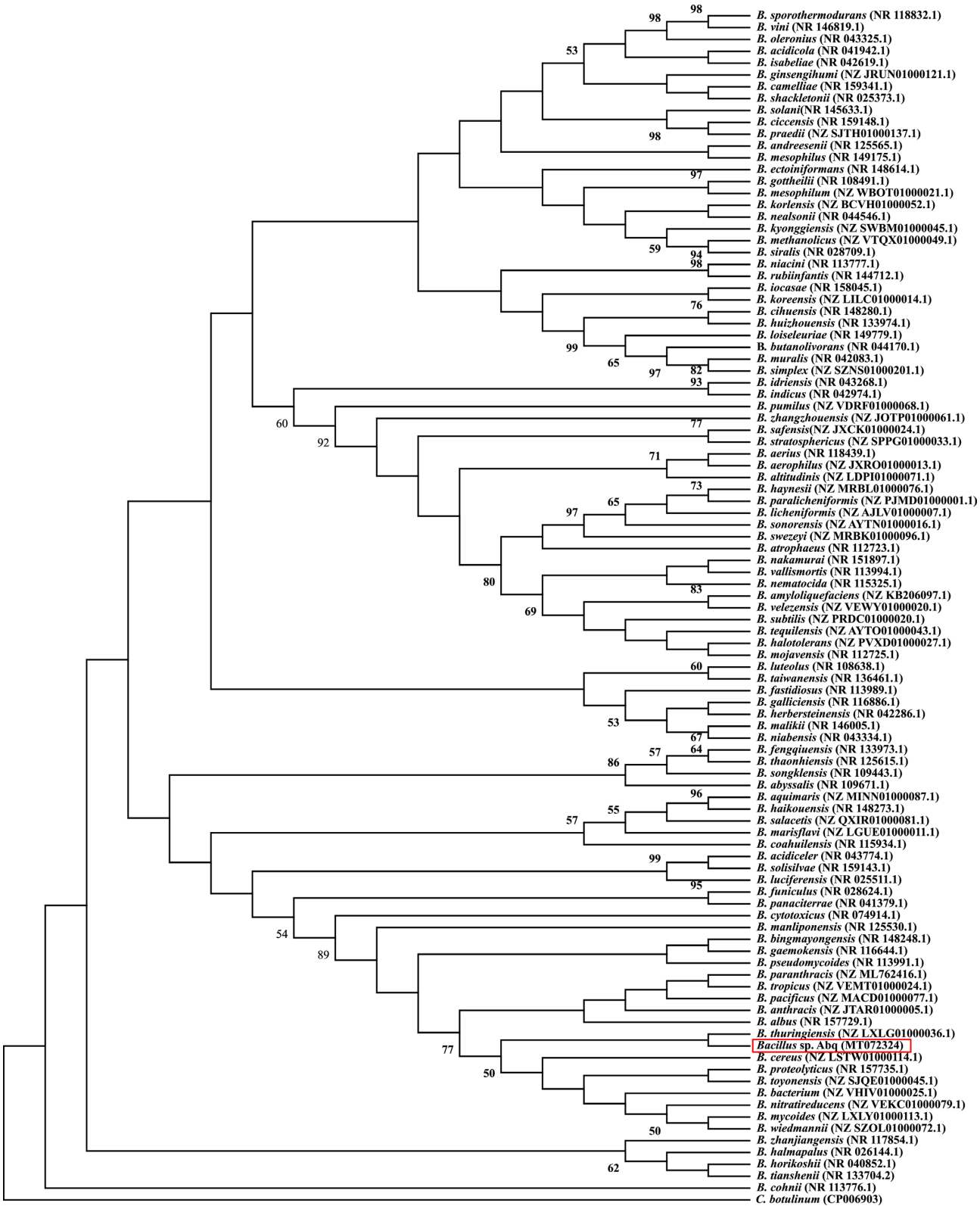

Figure 1. Phylogenetic tree for 16S rRNA sequence of *Bacillus* spp. GenBank accession number of the 16S rRNA sequences used for the phylogenetic analysis are given in parentheses. The tree with the highest log likelihood (-9369.02) is shown. Statistical support for the internal nodes was determined by 1000 bootstrap replicates and values of ≥50% are shown. The percentage of trees in which the associated taxa clustered together is shown next to the branches. The 16S rRNA of the *Bacillus* sp. Abq, analyzed in this study, is highlighted by a red rectangle.

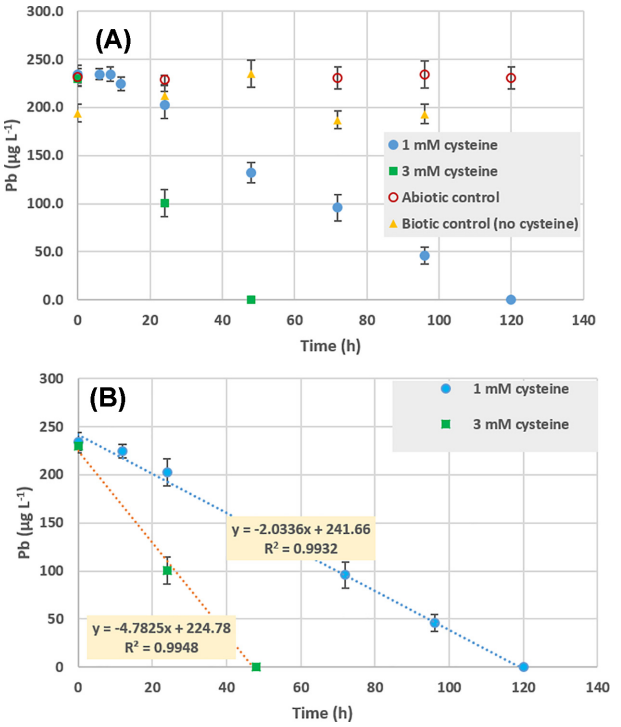

Figure 2. Lead removal by *Bacillus* sp. Abq under aerobic conditions. **(A)**, Removal of 1 mM Pb(II) in incubations amended with 1 mM and 3 mM cysteine. The abiotic control contains 1 mM Pb(II) and 1 mM cysteine. The biotic control without cysteine contains 1 mM Pb(II). The results represent the average of three replicates, δ<5%; **(B)**, Removal rates of 1 mM Pb(II) in solutions containing 1 mM and 3 mM cysteine. The removal rate of Pb(II) is the slope (a) of the equation y = ax + b. Growth conditions for (A) and (B): LB, oxic, initial pH 5.0, final pH ~7.5, 30°C, 150 rpm, dark.

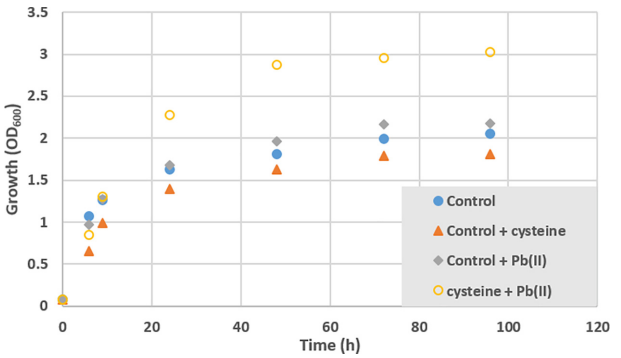

Figure 3. Growth of *Bacillus* sp. Abq under various conditions. Control represents the strain grown in LB; Control + cysteine contains 1 mM cysteine; control + Pb(II) contains 1 mM Pb(II); cysteine + Pb(II) represents the incubation containing 1 mM Pb(II) and 1 mM cysteine. Growth conditions: as described in Fig. 2.

assay and was compared to *Bacillus subtilis* ANT_WA51, a strain capable of surfactant production. *Bacillus* sp. Abq did not produce surfactants in any of the test conditions: in LB, in LB + Pb, and in LB + Pb + cysteine.

Lead (Pb) removal

Figure 2A presents the aerobic removal of lead by *Bacillus* sp. Abq in the presence of 1 mM and 3 mM cysteine. Using equimolar cysteine to Pb (1:1 ratio), the strain started to remove Pb from solution after the first 12 h of incubation (~4%), at which time point the removal increased with incubation time. 14% Pb was removed after 24 h, 44% after 48h, 59% after 72 h, 81% after 96 h, while at the last sampling point, 120 h, no Pb was detected in solution. Interestingly, using a 1:3 ratio Pb to cysteine, the Pb removal kinetics were accelerated, 56% removal after 24 h and no Pb measured in solution after 48 h. The start of Pb removal coincides with the mid-exponential phase of the bacterial growth (Fig. 3). The abiotic control using equimolar cysteine to Pb shows that lead is not removed during incubation, thus excluding the potential abiotic interactions leading to Pb(II) precipitation. On the other hand, the biotic control containing Pb(II) but without cysteine might indicate a slight Pb(II) removal that could be attributed to measurement errors or to the limited interaction of Pb(II) with bacterial biomass. As for removal rates, in the case of 1:1 ratio, Pb was removed at 2.03 µg L^{-1} h^{-1} (~8.7 µM L^{-1} h^{-1}), while in the case of 1:3 ratio, the removal rate increased to 4.78 µg L^{-1} h^{-1} (~20.4 µM L^{-1} h^{-1}) (Fig. 2B). By tripling the ratio of Pb to cysteine, the Pb removal rate only increased 2.35-fold (2.03 µg L^{-1} h^{-1} vs 4.78 µg L^{-1} h^{-1}). This indicates that the increase of the removal rate is not a linear process, leading to saturation for concentrations exceeding the equimolar ratio. In the case of the abiotic control (Pb + cysteine), Pb concentration remained constant in solution as a function of time. Overall, this set of results identifies cysteine as the causative agent of Pb removal from solution and *Bacillus* sp. Abq as the agent capable of using cysteine for this process.

The growth of *Bacillus* sp. Abq was measured under various conditions: the culture in LB, the culture in LB supplemented with 1 mM cysteine, the culture in LB supplemented with 1 mM Pb(II), and the culture in LB supplemented with 1 mM cysteine and 1 mM Pb(II). As a general observation, the culture supplemented with 1 mM cysteine and 1 mM Pb(II) displayed the highest optical density (OD) relative to the other three conditions that gave comparable results (Fig. 3). During the first 12 h of growth, the cultures produced similar optical densities; however, after this time point, the Pb(II) + cysteine incubation started to exhibit a higher OD than the other treatments. These results should be interpreted with caution because the formation of black PbS interferes with the proper OD measurement, thus not indicating a better growth of *Bacillus* sp. Abq when exposed to Pb(II) and cysteine. The important point is that the removal of Pb from solution is well correlated with the bacterial growth, confirming the biotically-driven lead transformation in this system. In order to exclude the possible chemical interaction of cysteine with Pb, we performed a series of experiments in LB and sterile distilled water at pH values relevant for the current study (pH 5, 7 and 9). The results did not indicate any formation of black PbS, nor the removal of Pb from solution (data not shown).

Pb(II) is suggested to cross the bacterial plasma membrane through non-specific uptake pathways for Mn(II) and Zn(II) (Jaroslawiecka and Piotrowska-Seget 2014). Bacteria have evolved efficient extracellular and intracellular defense mechanisms against lead toxicity. Lead can be sequestered outside the bacterial cell through its precipitation as insoluble phosphates or adsorption onto extracellular polysaccharides (Dopson *et al.* 2003). Lead sulfide has a very low solubility, $K_{sp} = 3.2 \times 10^{-28}$, second to phosphates, e.g. lead phosphate, $K_{sp} = 3 \times 10^{-44}$ (Rumble 2018). However, in view of the scarcity and essentiality of phosphorous for bacterial metabolism, the use of phosphates to sequester Pb(II) has marginally been reported (Chen *et al.* 2016).

In some instances, Pb(II) is pumped out from the cell by export systems using P-type ATPases which are distributed throughout bacteria (Rensing *et al.* 1998). These transporters

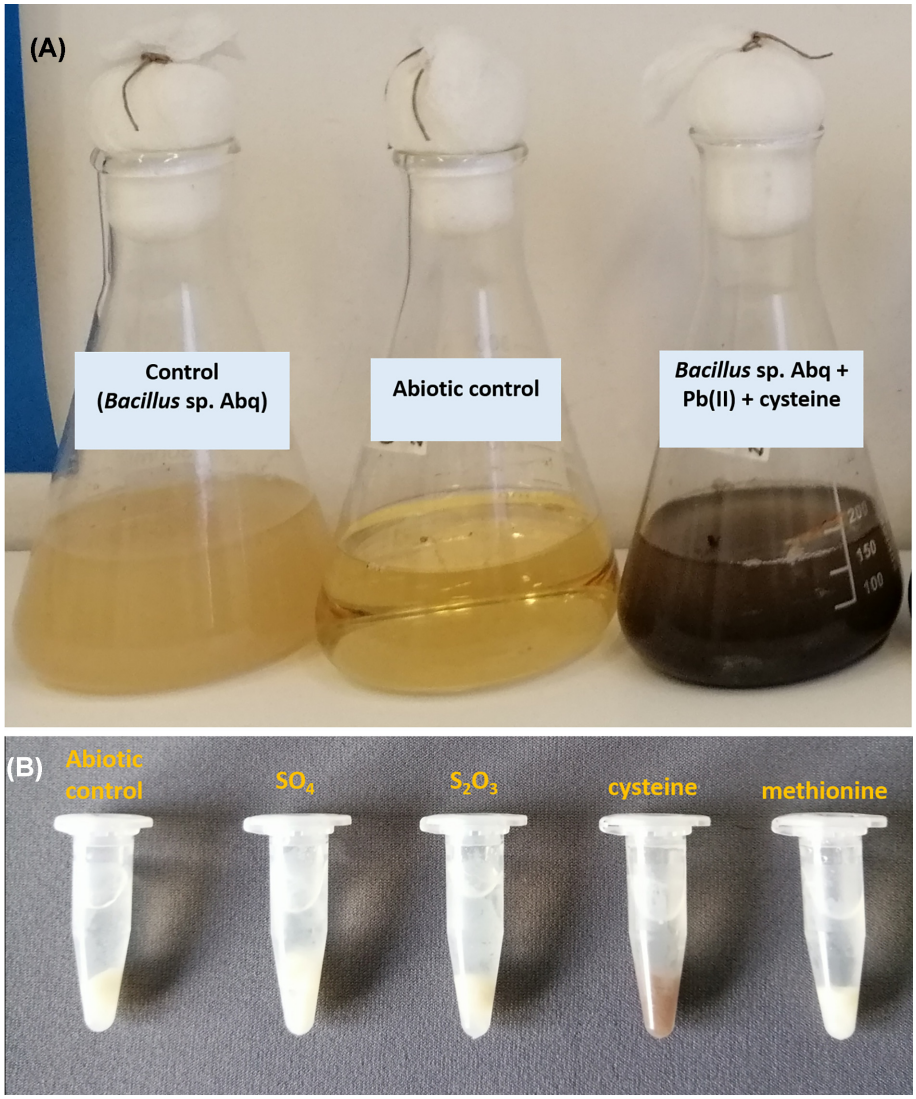

Figure 4. PbS formation by *Bacillus* sp. Abq under aerobic and anaerobic conditions. **(A)**, Aerobic incubation after 48 h in LB medium. The incubations were conducted under the same conditions as described in Fig. 2. The abiotic control contains LB, 1 mM Pb(II) and 1 mM cysteine, but without bacterial inoculum. **(B)**, Anaerobic incubation after 48 h in LB medium. The incubations were conducted at initial pH 7.0, final pH 7.5–8.0, 30°C, 150 rpm, dark. The abiotic control contains LB, 1 mM Pb(II) and 1 mM cysteine, but without bacterial inoculum. 1 mM SO_4, sulfate, S_2O_3, thiosulfate, and methionine were used under anoxic conditions.

include CadA, ZntA, and PbrA (Jaroslawiecka and Piotrowska-Seget 2014). Interestingly, these transporters appear to have an efficient crosstalk. For instance, when PbrA transporter was inactivated in *Cupriavidus metallidurans* CH34, the *zntA* and *cadA* increased their activity to complement for the loss of the former (Taghavi *et al.* 2009). Hynninen *et al.* (2009) documented a mixed detoxification mechanism where Pb(II) is first exported from the cytoplasm by PbrA and then is sequestered extracellularly as a phosphate salt using the inorganic phosphate produced by PbrB.

PbS formation under aerobic and anaerobic conditions

The formation of PbS under aerobic conditions in LB starts after 12 h of incubation and increases during incubation, accompanied by a progressive darkening of the solution (Fig. 4A). This indicates the progressive increase in PbS concentration with time, a result supported by the decrease in concentration of soluble Pb(II) (Fig. 2A). A separate experiment aimed to establish if cysteine can be degraded extracellularly by collecting the supernatant from a *Bacillus* sp. Abq culture grown using the same incubation conditions in LB medium amended with 1 mM cysteine was recovered. The supernatant was filter-sterilized and inoculated with 1 mM Pb(II), and with 1 mM Pb(II) + 1 mM cysteine. The incubations did not turn black and the Pb measurement did not indicate any Pb removal during the 7-day incubation period (data not shown). The abiotic control containing 1 mM Pb(II) and 1 mM cysteine indicates PbS cannot be formed. Since we could not perform the analysis on cysteine degradation as a function of incubation time, the decrease in Pb(II) concentration, the formation of PbS (characterized in detail below), as well as the control experiments, collectively indicate the contribution of cysteine as the source of H_2S and its intracellular degradation by *Bacillus* sp. Abq.

In a separate experiment, *Bacillus* sp. Abq was incubated in LB anaerobically (Fig. 4B). An abiotic control experiment containing LB medium amended with cysteine and Pb(II) was performed to exclude the possibility that the components of the

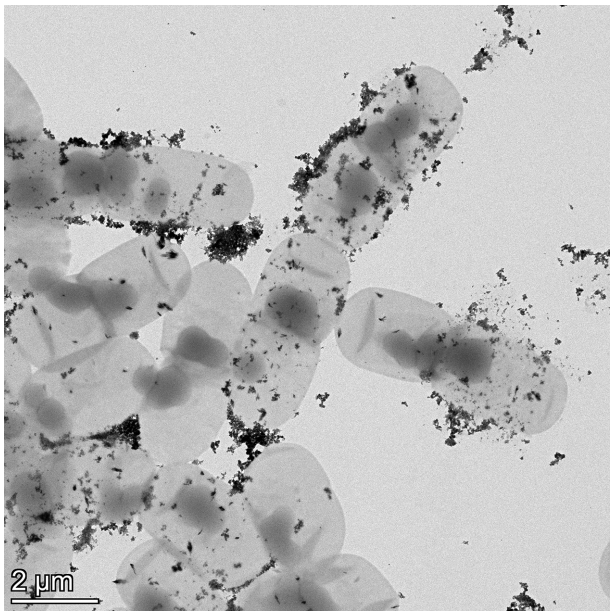

Figure 5. Bright-field TEM image showing dark clusters of PbS nanoparticles surrounding *Bacillus* sp. Abq formed under aerobic conditions. PbS nanoparticles are present in the extracellular environment and some are tightly attached to bacterial cells.

medium can react with Pb(II) forming PbS. The anaerobic experiment concluded that sulfide can only be formed by *Bacillus* sp. Abq in the presence of cysteine, as documented by the formation of a black precipitate (Fig. 4B). All other sulfur sources could not be used to generate H_2S. The formation of whitish precipitates in all other treatments, including the abiotic control experiment, indicates the formation of Pb(II) oxides at pH ~8.0. These results indicate that this strain was able to degrade cysteine anaerobically to H_2S. On the other hand, the possible use of sulfate and thiosulfate by *Bacillus* sp. Abq for anaerobic respiration can be ruled out (Barton and Fauque 2009).

PbS characterization

Low-magnification TEM images show cells surrounded by very fine-grained, crystalline material, producing dark contrast in bright-field images (Fig. 5). The nanoparticles occur extracellularly and attach to the cell membrane. In addition, particles also occur in some distance from the cells. According to EDS spectra obtained from clusters of the nanoparticles, they clearly contain Pb and S (Fig. 6C). Although the S K-peak overlaps with the Pb M-peaks, precluding an accurate quantitative evaluation of the composition, the presence of S is unambiguously shown by an analysis of the intensity profile (Fig. S2), additionally supporting the formation of extracellular PbS.

The spherical bacterial inclusions in Fig. 5 could be polyhydroxyalkanoate (PHA) granules. PHA serve as both a source of energy and as a carbon store (Shively *et al.* 2011), and various members of the genus *Bacillus* were shown to produce these inclusions (Singh, Patel and Kalia 2009). EDS analysis did not indicate the presence of Pb or S in the areas where these spots are present, thus excluding the possibility of Pb-containing intracellular accumulations. Due to the development of a black color during incubation, as a result of PbS formation, various staining techniques such as Sudan Black B, Nile Blue A or Nile Red could not have been applied to screen for the presence of PHA (Legat *et al.* 2010). Alternatively, these inclusions could be spores. The species belonging to the genus *Bacillus* can form spores under stressful conditions such as when exposed to toxic metals (Selenska-Pobell *et al.* 1999). The major limitation in evaluating the formation of spores during Pb(II) exposure was the production of black PbS which makes the use of various spore staining techniques (e.g. Schaeffer-Fulton stain using malachite green) inefficient.

Unequivocal identification of the Pb-bearing phase is possible by an analysis of electron diffraction patterns and high-resolution TEM images. SAED patterns obtained from clusters of nanoparticles show rings, suggesting that the material is crystalline but has a very fine (nm-scale) grain size, and the grains occur in random crystallographic orientations (Fig. S3, Supporting Information). The d-spacings corresponding to the rings are consistent with the structure of galena, PbS, and their relative intensities also match the features expected for galena (the most intense peak being at ~3 Å, the next strongest at ~2.1 Å, and the others being all very weak). HRTEM images of the nanoparticles show periodic fringes in most of them, indicating their crystalline character (Fig. 6A). The sizes of galena nanocrystals range from about 4 to 10 nm in this image. A Fourier transform (FT) calculated for the image shown in Fig. 6A (inset) displays only the rings corresponding to the structure of galena. A single nanoparticle (about 3 by 6 nm in size) is shown in Fig. 6B along with its FT; this particle is viewed along a major crystallographic axis, resulting in distinct spots in the FT that can be indexed on the basis of the galena structure. The composition of a cluster of PbS particles is confirmed by the EDS spectrum in Fig. 6C.

According to XRD data, the sample is dominated by lead sulfide, PbS (Fig. 7), with all detected peaks belonging to galena. The peaks on the diffractogram are slightly broad, which indicates the small (nm-scale) crystal size of the precipitate.

Model of cysteine degradation and extracellular PbS formation

Cysteine is the source of sulfur for the biosynthesis of a numerous cofactors such biotin, lipoic acid, molybdopterin and thiamine, as well as Fe-S clusters in proteins and thionucleosides in tRNA (Marquet 2001). Identifying the enzyme responsible for cysteine degradation was beyond the scope of this study. However, based on a literature survey briefly presented below, it appears no cysteine-degrading enzyme has been shown to be active extracellularly. For instance, cysteine desulfurase is an intracellular enzyme that catalyzes the conversion of *L*-cysteine to *L*-alanine and sulfane sulfur via the formation of a cysteine persulfide intermediate (Mihara and Esaki 2002). Cystathionine β-synthase was also found to produce H_2S upon reaction of cysteine in *Bacillus anthracis* (Devi *et al.* 2017). On the other hand, cysteine desulfhydrase catalyzes the conversion of *L*-cysteine to sulfide, ammonia, and pyruvate (Takagi and Ohtsu 2016). From this perspective, *Bacillus* sp. Abq seems to possess a cysteine desulhydrase or a cystathionine β-synthase able to release sulfide from cysteine. The formation of cysteine-Pb(II) complexes was reported at high pH values (9.1–10.4) and at mole ratios varying from 2.1 to 10.0, with $C_{Pb(II)} = 0.01$ and 0.1 M (Jalilehvand *et al.* 2015). The experimental conditions used in the current study do not support the possibility to form such complexes.

According to the available results, it is reasonable to conclude that cysteine is internalized by *Bacillus* sp. Abq, then enzymatically degraded at the intracellular level and a portion of the released sulfide is exported to the extracellular milieu as H_2S. Extracellularly, H_2S dissociates and sulfide reacts with Pb(II),

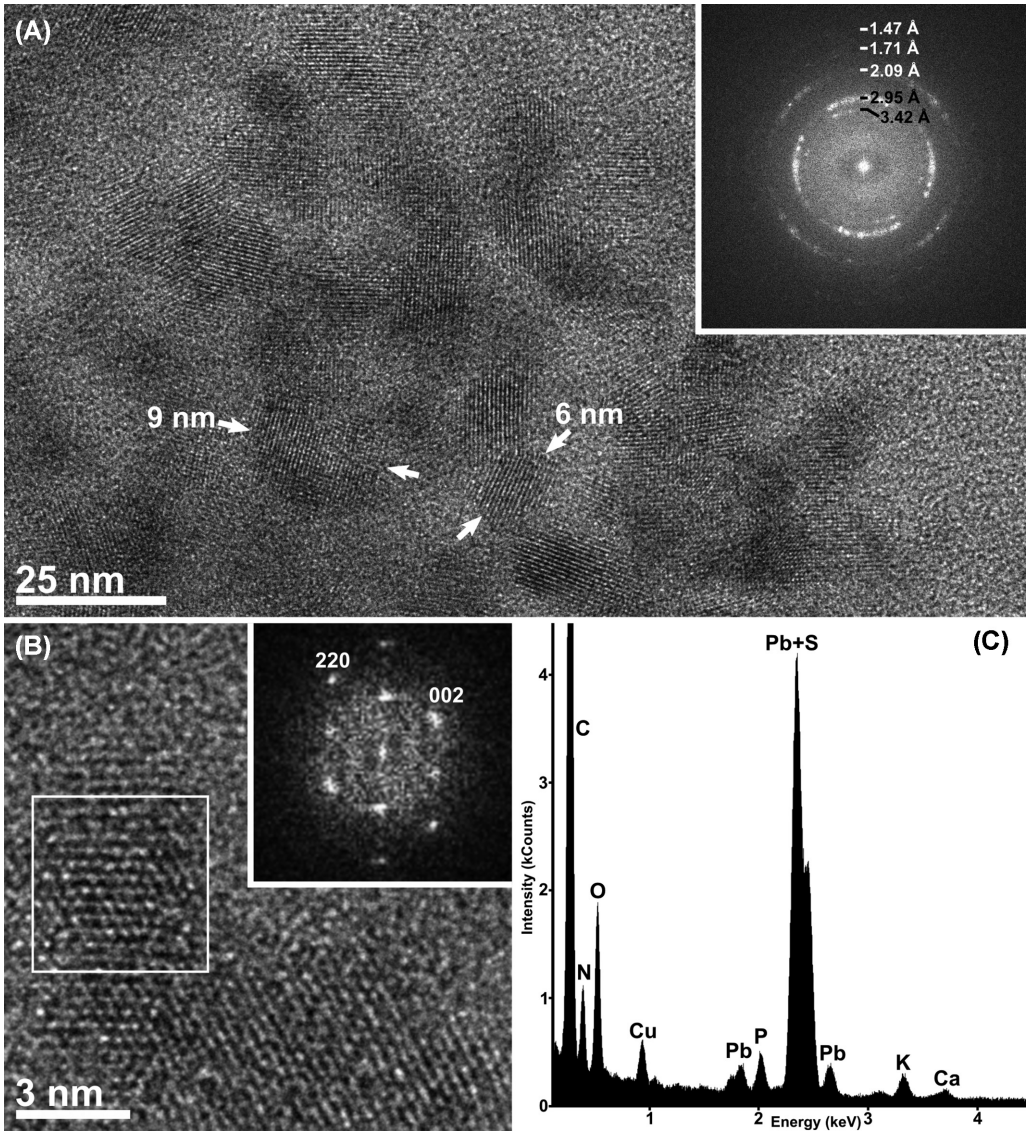

Figure 6. TEM analysis of biogenic PbS produced by *Bacillus* sp. Abq under aerobic conditions, **(A)**, HRTEM image of a cluster of randomly oriented nanocrystals and their Fourier Transform (FT, inset), in which the spatial frequencies in the nanocrystals are represented by intensity maxima producing rings. The diameters of the rings correspond to d-spacings as indicated by the green numbers, all of which are consistent with the structure of galena. **(B)**, HRTEM image and its FT (inset) of an individual galena nanocrystal, viewed with the electron beam parallel to the [1–10] crystallographic axis. **(C)**, EDS spectrum of biogenic PbS particles produced by *Bacillus* sp. Abq under aerobic conditions. The spectrum shows the presence of Pb and S in addition to C, N, O and minor P, K, and Ca. The Cu peak is an artifact from the TEM support grid.

yielding PbS (Fig. 8). H_2S has an acid dissociation constant, pKa ~7.0 (Rumble 2018). The extracellular transfer of H_2S to react with Pb(II) is further supported by Fig. S4 (Supporting Information) showing a brown halo surrounding bacterial colonies grown aerobically on Pb and cysteine containing media.

The model of Pb(II) precipitation using cysteine by *Bacillus* sp. Abq is supported by the following results: (i) Pb is removed as a function of incubation time (Fig. 2A), (ii) Cysteine is the source of sulfide used for PbS precipitation (Fig. 4), (iii) Increasing cysteine concentration accelerates Pb removal rate, (iv) PbS particles form extracellularly (Fig. 5) and (v) A brown halo forms outside bacterial colonies, indicating the release of sulfide and the precipitation of PbS (Fig. S4, Supporting Information).

Because Pb is toxic for bacteria, sequestering it as a low solubility mineral offers the advantage of neutralizing its toxicity. Cysteine is a critical amino acid for bacterial metabolism, being an important stock molecule, and taken from the environment or/and synthesized endogenously from serine (Takagi and Ohtsu 2016). The limited choice of *Bacillus* sp. Abq for cysteine as a strategy for Pb precipitation might be explained in the nature of this amino acid itself. Sulfur is present in cysteine as sulfide, a highly reactive valence state with high affinity for metals (Staicu *et al.* 2019). Consequently, the possibility to readily obtain sulfide from cysteine, bypassing the time-consuming production of S^{2-} from high-valence states of sulfur (e.g. sulfate, sulfite, thiosulfate), might help bacteria to counteract Pb toxicity in a fast and efficient manner. It is noteworthy to mention that H_2S has been reported to act as a universal defense against antibiotics in bacteria (Shatalin *et al.* 2011) and is exported to the extracellular milieu by diffusion (Mathai *et al.* 2009).

It is possible that initially Pb(II) enters the cell and triggers a detoxification reaction by pumping out Pb(II) ions. However, this

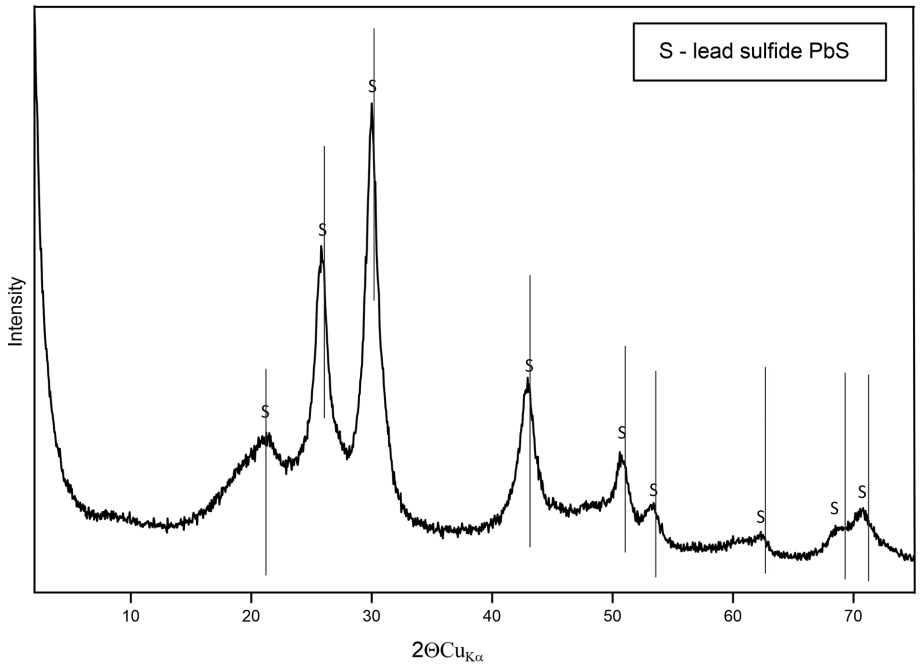

Figure 7. XRD of biogenic PbS produced by *Bacillus* sp. Abq under aerobic conditions.

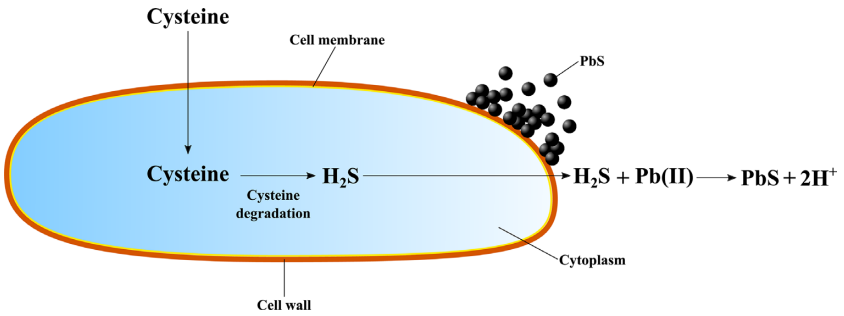

Figure 8. Model of Pb detoxification in *Bacillus* sp. Abq using cysteine and forming low-solubility PbS. Figure not drawn to scale.

strategy is both energy intensive and not efficient on medium and long term since Pb(II) can enter in the cell again. The use of cysteine as a feedstock for sulfide could be the second response mechanism of bacteria, as forming an insoluble mineral outside the cell renders Pb non-bioavailable. Roane (1999) documented the formation of Pb precipitates intracellularly (*Bacillus megaterium*) and extracellularly (*Pseudomonas marginalis*). However, the study did not investigate the mineralogical nature of the two precipitates, while in the case of *P. marginalis* it was hypothesized the involvement of an exopolymer in the sequestration of Pb.

Biomineralization process of PbS: Resource recovery perspectives

Lead is used on large scale by various industrial applications, generating waste materials (e.g. wastewater) charged with significant amounts of Pb. If not properly treated, Pb will be released to the environment leading to pollution and biodiversity loss (Brink, Horstmann and Peens 2019). Such an industrial effluent is spent lead-acid battery wastewater, a matrix containing high levels of sulfate (grams L^{-1}) and Pb (<5 mg L^{-1}) (Vu *et al.* 2019). Most of the studies investigating this industrial wastewater type only focused on its treatment, while the resource recovery component was not taken into consideration. Importantly, PbS (galena) is currently the main source of lead production using pyrometallurgical processes (Rumble 2018). Because Pb is present in spent lead-acid battery wastewater in its soluble form, Pb(II), PbS formation offers the advantage of efficient recovery in the form of a solid product. Moreover, recovering PbS from a secondary resource would contribute to reducing the pressure on natural resources in the framework of circular economy (Cordoba and Staicu 2018; Kisser *et al.* 2020). The purity of the recovered biogenic PbS is in contrast with the mined minerals which are mixed with other minerals and gangue. Pyrometallurgical processes for Pb production are energy intensive and require numerous production phases, entailing additional costs and environmental degradation. The increased demand for metals using finite resources makes recycling of secondary resources critical in the near future (Vidal *et al.* 2017).

CONCLUSION

This study documented a novel precipitation strategy used by *Bacillus* sp. Abq, a novel strain isolated from an aquifer in New Mexico, USA and belonging to *Bacillus cereus* sensu lato, against lead (Pb) by means of degrading cysteine and extracellularly precipitating PbS (galena). The experimental dataset supports the

model of cysteine import from the growth media, active degradation of cysteine at the intracellular level and the export of sulfide, moiety released from this amino acid, followed by the precipitation of Pb as highly insoluble and non-bioavailable PbS. One significant finding is the narrow size of PbS, <10 nm, and its exclusive extracellular biomineralization. Its extracellular distribution is indicative of an efficient system that prevents the reentering of toxic Pb in the cell. Biogenic PbS is crystalline and shows a high degree of purity when compared with reference materials. Because PbS is currently the main source of Pb industrial production, this study might open the possibility to biologically recover galena from Pb-laden wastewaters and use it as feedstock instead, replacing raw and limiting materials. From a microbial ecology perspective, identifying new pathways used by bacteria to precipitate Pb(II) would serve to decontaminate industrially-polluted soils that are a legacy of past heavy industrial activity using a non-invasive, eco-friendly treatment approach. Additionally, understating the microbial metabolism of Pb is crucial in man-made infrastructures such as the aging water supply systems made of lead conduits (e.g. the lead poisoning event in Flint, Michigan). In a follow up study, we plan to investigate the potential of this bacterial isolate to precipitate other toxic metals (e.g. Cd) using cysteine, therefore exploring its full potential to form non-toxic and chemically stable metal sulfides.

SUPPLEMENTARY DATA

Supplementary data are available at FEMSEC online.

ACKNOWLEDGMENTS

LS and PJW acknowledge the National Science Centre (NCN), Poland, Grant number 2017/26/D/NZ1/00408, for financial support. LS acknowledges Dr Alina Maria Holban (University of Bucharest, Romania), Prof Hisaaki Mihara (Ritsumeikan University, Japan) and Dr Rob van Houdt (Belgian Nuclear Research Centre, Belgium) for productive discussions. FLJ was supported by a Patricia Robert-Harris fellowship and the research was supported, in part, by a grant to LLB from the US Department of Energy through the Waste-Management Education and Research Consortium and the Sandia National Laboratories under Contract DE-AC04–90AL8500. The authors acknowledge Tomasz Bajda (AGH-KGHM, Krakow) for help with XRD analysis and Bartosz Rewerski (UW) for Pb analysis. The authors recognize Belinda Ramirez and Nada Kherbik for technical assistance in this project. TEM studies were performed at the Nanolab of the University of Pannonia, using Grants no. GINOP-2.3.3–15-2016–0009 and GINOP-2.3.2–15-2016–00017 from the European Structural and Investments Funds and the Hungarian Government.

Conflicts of interests. None declared.

REFERENCES

Barton LL, Fauque GD. Biochemistry, physiology and biotechnology of sulfate-reducing bacteria. *Adv Appl Microbiol* 2009;**68**:41–98.

Brink HG, Horstmann C, Peens J. Microbial Pb(II)-precipitation: the influence of oxygen on Pb(II)-removal from aqueous environment and the resulting precipitate identity. *Int J Environ Sci Technol* 2019;**17**:409–20.

Bruins MR, Kapil S, Oehme FW. Microbial resistance to metals in the environment. *Ecotoxicol Environ Saf* 2000;**45**:198–207.

Campaner VP, Luiz-Silva W, Machado W. Geochemistry of acid mine drainage from a coal mining area and processes controlling metal attenuation in stream waters, southern Brazil. *An Acad Bras Cienc* 2014;**86**:539–54.

Canfield RL, Henderson CR, Jr, Cory-Slechta DA *et al.* Intellectual impairment in children with blood lead concentrations below 10 microg per deciliter. *N Engl J Med* 2003;**348**:1517–26.

Chen Z, Pan X, Chen H *et al.* Biomineralization of Pb(II) into Pb-hydroxyapatite induced by *Bacillus cereus* 12-2 isolated from lead-zinc mine tailings. *J Hazard Mat* 2016;**301**:531–37.

Cordoba P, Staicu LC. Flue Gas Desulfurization effluents: an unexploited selenium resource. *Fuel* 2018;**223**:268–76.

Devi S, Abdul Rehman SA, Tarique KF *et al.* Structural characterization and functional analysis of cystathionine beta-synthase: an enzyme involved in the reverse transsulfuration pathway of *Bacillus anthracis*. *FEBS J* 2017;**284**:3862–80.

Dopson M, Baker-Austin C, Koppineedi PR *et al.* Growth in sulfidic mineral environments: metal resistance mechanisms in acidophilic micro-organisms. *Microbiology* 2003;**149**:1959–70.

Finlay NC, Peacock CL, Hudson-Edwards KA *et al.* Characteristics and mechanisms of Pb(II) sorption onto Fe-rich waste water treatment residue (WTR): A potential sustainable Pb immobilisation technology for soils. *J Hazard Mater* 2021;**402**:123433.

Fu F, Wang Q. Removal of heavy metal ions from wastewater: a review. *J Environ Manage* 2011;**92**:407–18.

Hynninen A, Touzé T, Pitkänen L *et al.* An efflux transporter PbrA and a phosphatase PbrB cooperate in a lead-resistance mechanism in bacteria. *Mol Microbiol* 2009;**74**:384–94.

Jahan R, Bodratti AM, Tsianou M *et al.* Biosurfactants, natural alternatives to synthetic surfactants: Physicochemical properties and applications. *Adv Colloid Interface Sci* 2020;**275**:102061.

Jalilehvand F, Sisombath NS, Schell AC *et al.* Lead(II) complex formation with L-cysteine in aqueous solution. *Inorg Chem* 2015;**54**:2160–70.

Jaroslawiecka A, Piotrowska-Seget Z. Lead resistance in micro-organisms. *Microbiology* 2014;**160**:12–25.

Jensen GB, Hansen BM, Eilenberg J *et al.* The hidden lifestyles of *Bacillus cereus* and relatives. *Environ Microbiol* 2003;**5**:631–40.

Kisser J, Wirth M, De Gusseme *et al.* A review of nature-based solutions for resource recovery in cities. *Blue-Green Systems* 2020;**2**:138–72.

Kumar S, Stecher G, Li M *et al.* MEGA X: Molecular Evolutionary Genetics Analysis across computing platforms. *Mol Biol Evol* 2018;**35**:1547–49.

Legat A, Gruber C, Zangger K *et al.* Identification of polyhydroxyalkanoates in Halococcus and other haloarchaeal species. *Appl Microbiol Biotechnol* 2010;**87**:1119–27.

Marquet A. Enzymology of carbon-sulfur bond formation. *Curr Opin Chem Biol* 2001;**5**:541–49.

Mathai JC, Missner A, Kugler P *et al.* No facilitator required for membrane transport of hydrogen sulfide. *Proc Natl Acad Sci* 2009;**106**:16633–38.

Mihara H, Esaki N. Bacterial cysteine desulfurases: their function and mechanisms. *Appl Microbiol Biotechnol* 2002;**60**:12–23.

Mills C, Simpson I, Adderley WP. The lead legacy: the relationship between historical mining, pollution and the post-mining landscape. *Landsc Hist* 2014;**35**:47–72.

Morikawa M. Beneficial biofilm formation by industrial bacteria *Bacillus subtilis* and related species. *J Biosci Bioeng* 2006;**101**:1–8.

Muyzer G, Stams AJM. 2008. The ecology and biotechnology of sulphate-reducing bacteria. *Nat Rev Microbiol* 2008;**6**:441–54.
Needleman H. Lead poisoning. *Annu Rev Med* 2004;**55**:209–22.
Rensing C, Sun Y, Mitra B *et al*. Pb(II)-translocating P-type ATPases. *J Biol Chem* 1998;**273**:32614–17.
Roane TM. Lead resistance in two bacterial isolates from heavy metal-contaminated soils. *Microb Ecol* 1999;**3**:218–24.
Roy S, Edwards MA. Preventing another lead (Pb) in drinking water crisis: Lessons from the Washington D.C. and Flint MI contamination events. *Curr Opin Environ Sci Health* 2018;**7**: 34–44.
Rumble JR. *CRC Handbook of Chemistry and Physics*, 99th ed. Boca Raton: CRC Press, 2018.
Selenska-Pobell SP, Panak V, Miteva I *et al*. Selective accumulation of heavy metals by three indigeneous *Bacillus* strains, *B. cereus*, *B. megaterium* and *B. sphaericus* from drain waters of a uranium waste pile. *FEMS Microbiol Ecol* 1999;**29**:59–67.
Shatalin K, Shatalina E, Mironov A *et al*. H2S: a universal defense against antibiotics in bacteria. *Science* 2011;**334**:986.
Shively JM, Cannon GC, Heinhorst S *et al*. *Bacterial and Archaeal inclusions*. *In: Encyclopedia of Life Sciences*. Chichester: John Wiley & Sons, 2011.
Sigma. https://www.sigmaaldrich.com/content/dam/sigma-aldrich/docs/Sigma-Aldrich/Datasheet/1/44940dat.pdf (15 January 2020, date last accessed).
Singh M, Patel S, Kalia V. *Bacillus subtilis* as potential producer for polyhydroxyalkanoates. *Microb Cell Fact* 2009;**8**:38.
Staicu LC, Simon S, Guibaud G *et al*. Biogeochemistry of trace elements in anaerobic digesters. In: Fermoso FF *et al*. (eds.). *Trace elements in anaerobic biotechnologies*. London: IWA, 2019, 23–50.
Taghavi S, Lesaulnier C, Monchy S *et al*. Lead(II) resistance in *Cupriavidus metallidurans* CH34: interplay between plasmid and chromosomally-located functions. *Anton Leeuw Int J G* 2009;**96**:171–82.
Takagi H, Ohtsu I. L-cysteine metabolism and fermentation in microorganisms. *Adv Biochem Eng Biotechnol* 2016;**159**: 129–51.
Tamura K, Nei M. Estimation of the number of nucleotide substitutions in the control region of mitochondrial DNA in humans and chimpanzees. *Mol Biol Evol* 1993;**10**: 512–26.
Vidal O, Rostom F, Francois C *et al*. Global trends in metal consumption and supply: the raw material-energy nexus. *Elements* 2017;**13**:319–24.
Vu HH, Gu S, Thriveni T *et al*. Sustainable treatment for sulfate and lead removal from battery wastewater. *Sustainability* 2019;**11**:3497.
Wedge A. Lead. In: *Air pollution and health*. In: Maynard R *et al*. (eds.). Academic Press, 1999, 797–812.

Supplementary Material

PbS biomineralization using cysteine: *Bacillus cereus* and the sulfur rush

Lucian C. Staicu[1,*], Paulina J. Wojtowicz[1], Mihály Pósfai[2], Péter Pekker[3], Adrian Gorecki[1], Fiona L. Jordan[4], and Larry L. Barton[4]

[1]Faculty of Biology, University of Warsaw, Miecznikowa 1, 02-096 Warsaw, Poland

[2]Department of Earth and Environmental Sciences, University of Pannonia, Egyetem u. 10, H-8200, Veszprém, Hungary

[3]Research Institute of Biomolecular and Chemical Engineering, University of Pannonia, Egyetem u. 10, H-8200, Veszprém, Hungary

[4]Department of Biology, University of New Mexico, MSCO3 2020, Albuquerque NM 87131, USA

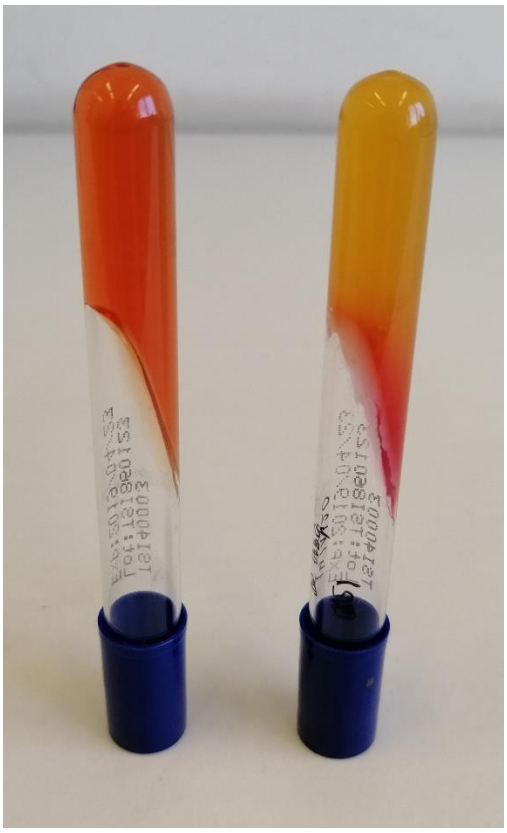

Figure S1. Triple Sugar Agar (TSI) test. Left (control, uninoculated slant), right (slant inoculated with *Bacillus* sp. Abq). The bottom of the tube turned yellow, indicative of glucose fermentation. The fact no darkening appeared in the inoculated tube shows the incapacity of *Bacillus* sp. Abq to reduce sulfate and thiosulfate to hydrogen sulfide, that would have reacted with the Fe(II) present in TSI, thus forming a black iron sulfide mineral precipitate.

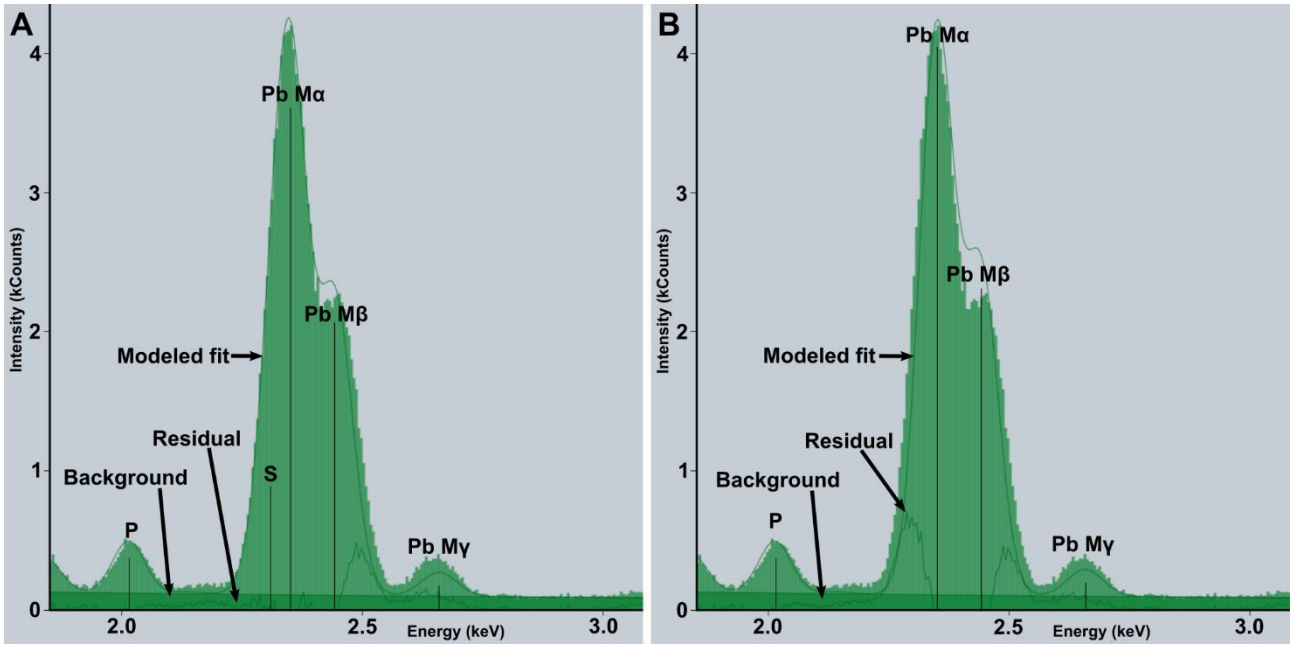

Figure S2. Analysis of the family of M-peaks produced by Pb in an EDS spectrum obtained from a cluster of nanocrystals. Both graphs show a raw spectrum with a fitted background, a modeled curve fitted to the peaks, and a curve for the residual intensity (the remaining intensity after subtracting the modeled value from the net intensity), as indicated in the graph. (a) Modeled fit with S present; (b) modeled fit with S absent; as seen from the higher values of the residual curve in (b), modeling with S present produces a far better result, suggesting the particles contain both Pb and S.

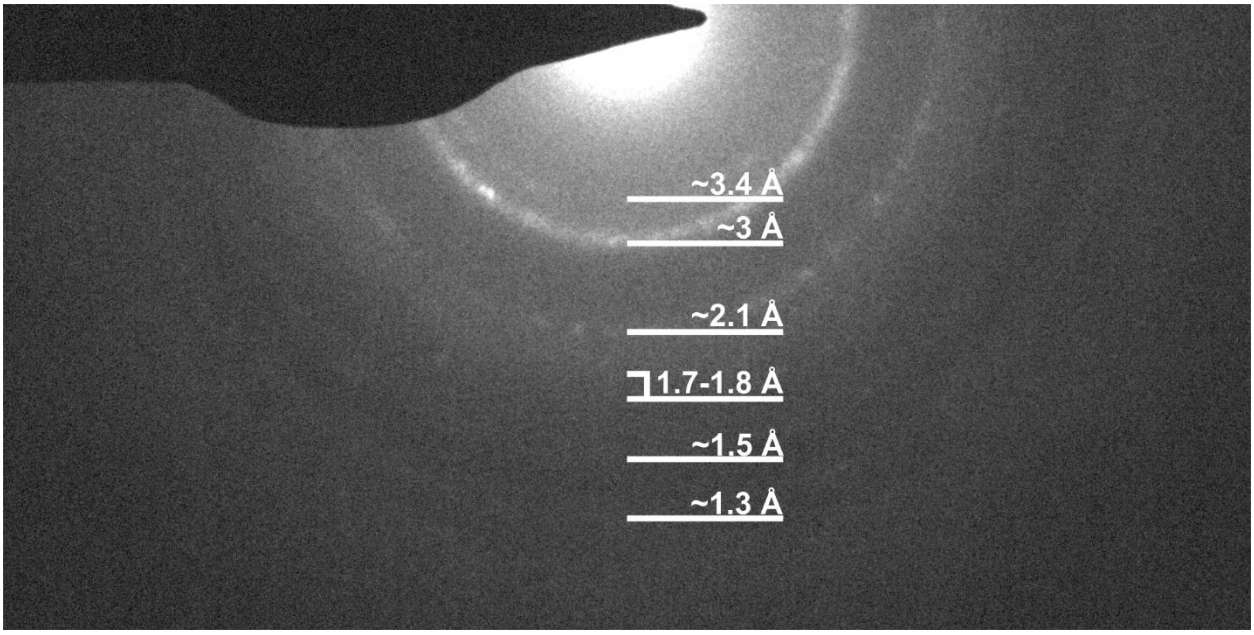

Figure S3. Selected-area electron diffraction pattern of a cluster of Pb-bearing nanocrystals. The rings indicate that the particles are crystalline and occur in random crystallographic orientations. The rings correspond to distinct periodicities (d-spacings) in the crystals, as shown by the values (in Å) written on them. All d-spacings and their relative intensities are consistent with the structure of galena, PbS.

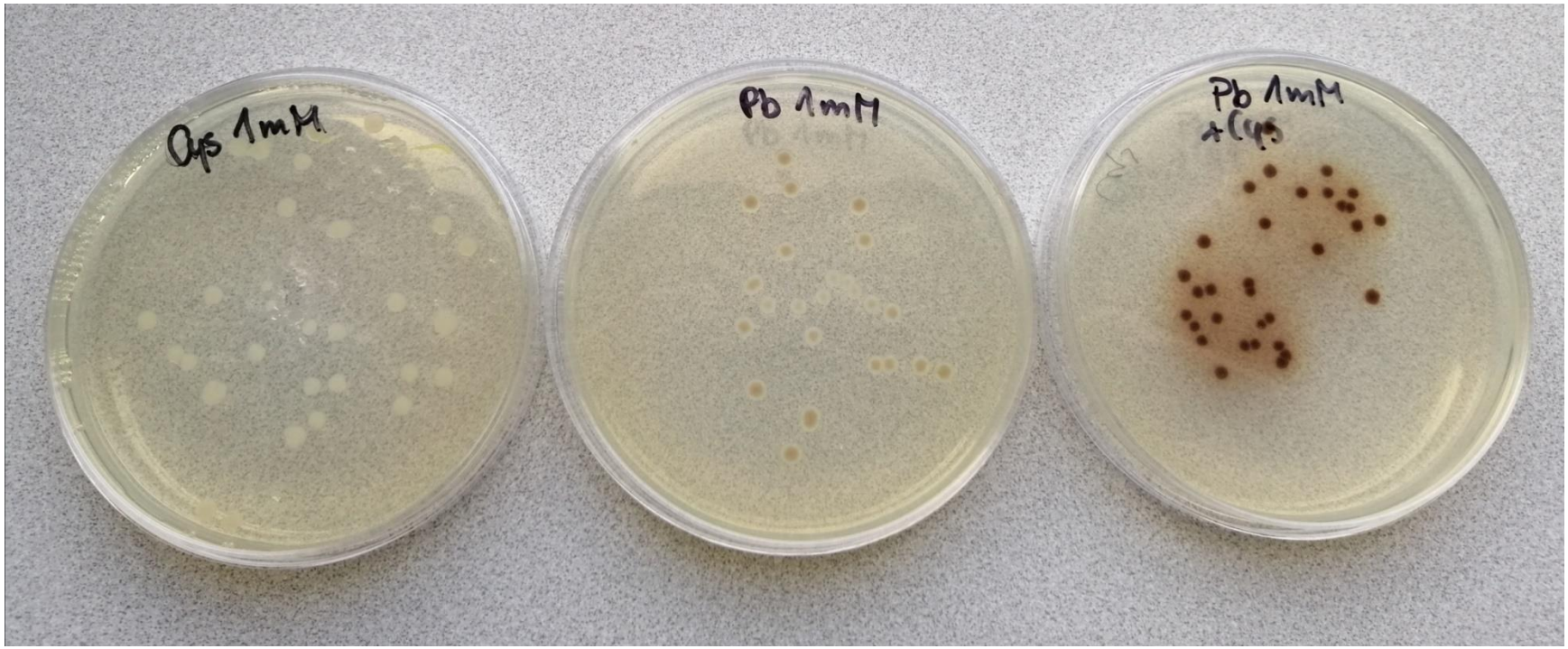

Figure S4. Growth of *Bacillus* sp. Abq on agar-LB plates containing 1mM cysteine, 1 mM Pb(II), and 1 mM cysteine + 1 mM Pb(II). The brown halo on the third plate supports the hypothesis that sulfide is exported outside bacterial colonies where it reacts with Pb(II) forming black PbS.

Table S1. Biochemical characterization of *Bacillus* sp. Abq (+, positive reaction; -, negative reaction).

API 20E		Incubation time		API 20NE		Incubation time	
Acronym	**Enzyme**	**24h**	**48h**	**Acronym**	**Enzyme**	**24h**	**48h**
ONPG	ß-galactosidase	-	-	NO_3	Nitrate reduction to NO_2	+	+
ADH	Arginine dihydrolase	-	+	TRP	Indole production (TRyptoPhane)	-	-
LDC	Lysine decarboxylase	-	-	GLU	D-glucose fermentation	-	+
ODC	Ornithine decarboxylase	-	-	ADH	L-Arginine dihydrolase	+	+
CIT	Citrate utilization	-	+	URE	Urease	-	-
H_2S	Hydrogen sulfide production (from thiosulfate)	-	-	ESC	Hydrolysis (ß-glucosidase) (ESCulin)	+	+
URE	Urease	-	-	GEL	Hydrolysis (protease) (GELatin)	+	+
TDA	Tryptophan deaminase	+	+	PNPG	4-Nitrophenyl-β-D- glucopyranoside	-	-
IND	Indole production	-	-	GLU	Assimilation (GLUcose)	+	+
VP	Acetoin production	-	-	ARA	Assimilation (ARAbinose)	-	-
GEL	Gelatinase	+	+	MNE	Assimilation (ManNosE)	-	-
GLU	Glucose fermentation/oxidation	+	+	MAN	Assimilation (MANnitol)	-	-
MAN	D-Mannitol fermentation/oxidation	-	-	NAG	Assimilation (N-Acetyl-Glucosamine)	+	+
INO	Inositol fermentation/oxidation	-	-	MAL	Assimilation (MALtose)	+	+

SOR	D-Sorbitol fermentation/oxidation	-	-	GNT	Assimilation (potassium GlucoNate)	+	+
RHA	L-Rhamnose fermentation/oxidation	-	-	CAP	Assimilation (CAPric acid)	-	-
SAC	D-Saccharose fermentation/oxidation	-	-	ADI	Assimilation (ADIpic acid)	-	-
MEL	D-Melibiose fermentation/oxidation	-	-	MLT	Assimilation (MaLaTe)	+	+
AMY	Amygdaline fermentation/oxidation	-	-	CIT	Assimilation (trisodium CITrate)	-	+
ARA	L-Arabinose fermentation/oxidation	-	-	PAC	Assimilation (PhenylACetic acid)	-	-